

# The crystal structure of pararobertsite and its relationship to mitridatite

ANTHONY R. KAMPF\*

Natural History Museum of Los Angeles County, 900 Exposition Boulevard, Los Angeles, California 90007, U.S.A.

## ABSTRACT

The crystal structure of pararobertsite,  $\text{Ca}_2(\text{H}_2\text{O})_2[\text{Mn}^{3+}_2\text{O}_2(\text{PO}_4)_3] \cdot \text{H}_2\text{O}$ ,  $P2_1/c$ ,  $a = 8.814(4)$ ,  $b = 13.233(5)$ ,  $c = 11.056(4)$  Å,  $\beta = 101.184(7)^\circ$ ,  $V = 1265.0(9)$  Å<sup>3</sup>,  $Z = 4$  has been solved by direct methods and refined to  $R = 0.042$  for 1319  $F_o > 4\sigma(F_o)$  using  $\text{MoK}\alpha$  X-ray data. In the structure of pararobertsite, Z-shaped edge-sharing chains of  $\text{Mn}^{3+}\text{O}_6$  octahedra link to one another via shared O vertices and  $\text{PO}_4$  tetrahedra to form a compact sheet of composition  $\frac{2}{3}[\text{Mn}^{3+}_2\text{O}_2(\text{PO}_4)_3]^{4-}$  oriented parallel to  $\{100\}$ . The space between the compact sheets is filled with a thick open assemblage of  $\text{CaO}_5(\text{H}_2\text{O})_2$  polyhedra and isolated water molecules. The structure bears strong similarities to the mitridatite ( $\text{Fe}^{3+}$ ) structure and, therefore, to its robertsite ( $\text{Mn}^{3+}$ ) isotype.

## INTRODUCTION

The mineral pararobertsite from from the Tip Top pegmatite, Custer County, South Dakota was described by Roberts et al. (1989), who named the mineral for its close chemical and crystallographic relationship to robertsite,  $\text{Ca}_6(\text{H}_2\text{O})_6[\text{Mn}^{3+}_3\text{O}_6(\text{PO}_4)_9] \cdot 3\text{H}_2\text{O}$  in the asymmetric unit,  $Z = 4$ . Robertsite is isostructural with mitridatite,  $\text{Ca}_6(\text{H}_2\text{O})_6[\text{Fe}^{3+}_3\text{O}_6(\text{PO}_4)_9] \cdot 3\text{H}_2\text{O}$ , whose structure was determined by Moore and Araki (1977). This study was undertaken to elucidate the structural relationship between pararobertsite and robertsite.

## STRUCTURE DETERMINATION

Single-crystal X-ray precession and diffractometer studies showed pararobertsite to be monoclinic, space group  $P2_1/c$ ,  $a = 8.814(4)$ ,  $b = 13.233(5)$ ,  $c = 11.056(4)$  Å,  $\beta = 101.184(7)^\circ$ ,  $V = 1265.0(9)$  Å<sup>3</sup>,  $Z = 4$ . The cell parameters were refined from the peak positions obtained from the structure data collection. These cell parameters compare closely to those reported by Roberts et al. (1989),  $a = 8.825$ ,  $b = 13.258$ ,  $c = 11.087$  Å,  $\beta = 101.19^\circ$ .

X-ray intensity data were collected from a thin tabular crystal of pararobertsite of dimensions  $0.14 \times 0.11 \times 0.01$  mm<sup>3</sup> using a Bruker PLATFORM 3-circle goniometer equipped with a 1 K SMART CCD detector. The operating conditions were: room temperature, 50 kV, 45 mA, graphite-monochromatized  $\text{MoK}\alpha$  radiation ( $\lambda = 0.71069$  Å). Frame widths of  $0.3^\circ$  in  $\omega$  were used to acquire each frame for 120 s. A total of 1271 frames of data was collected, providing a half sphere of three-dimensional data. Data were collected for  $4.7^\circ \leq 2\theta \leq 56.6^\circ$ . Fifty duplicate frames acquired at the end of the data collection indicated that no significant decay had taken place. The 7946 measured intensities ( $\bar{1}1 \leq h \leq 11$ ,  $\bar{1}3 \leq k \leq 17$ ,  $\bar{1}4 \leq l \leq 14$ ) were corrected for Lorentz and polarization effects using the program SAINT and an empirical absorption correction was applied using the

program SADABS. The final data set reduced to 3014 unique reflections. The absorption correction lowered  $R_{\text{INT}}$  from 3.8 to 3.1%.

The SHELXL97 software (Sheldrick 1997) was used for the determination and refinement of the structure. The metal atoms (Ca, Mn, and P) and several of the O atoms were readily located by direct methods. The positions of the remaining O atoms were obtained from subsequent difference-Fourier syntheses. In subsequent refinement cycles, anisotropic displacement parameters for all non-hydrogen atoms were refined to a conventional  $R$  index of 0.043 and  $wR_2 = 0.105$  [weighted  $R$  factor on  $F^2$ , as defined by Sheldrick (1997)] for 1319 measured reflections with  $F_o > 4\sigma(F_o)$ ,  $R = 0.137$  and  $wR_2 = 0.153$  for all 3014 data, and goodness of fit = 0.619. At this point examination of the highest peaks in the difference-Fourier synthesis coupled with valence-bond and geometrical considerations allowed the location of all H atoms. With H atom positions and isotropic displacement parameters (= 0.05) held invariant, the final refinement cycles yielded  $R = 0.042$  and  $wR_2 = 0.099$  for 1319 measured reflections with  $F_o > 4\sigma(F_o)$ ,  $R = 0.136$  and  $wR_2 = 0.149$  for all 3014 reflections, and goodness of fit = 0.601. Maximum and minimum heights in the final difference Fourier synthesis were  $+1.15$  and  $-0.76$  e/Å<sup>3</sup>.

Table 1 includes the final fractional coordinates and displacement parameters, Table 2<sup>1</sup> the observed and calculated structure factors, Table 3 interatomic distances and angles, and Table 4 the bond valences.

## DESCRIPTION OF THE STRUCTURE AND COMPARISON TO MITRIDATITE

In the structure of pararobertsite, Z-shaped edge-sharing chains of  $\text{Mn}^{3+}\text{O}_6$  octahedra link to one another via shared O vertices and  $\text{PO}_4$  tetrahedra to form a compact sheet of composition  $\frac{2}{3}[\text{Mn}^{3+}_2\text{O}_2(\text{PO}_4)_3]^{4-}$  oriented parallel to  $\{100\}$  (Fig. 1a). (The notation  $\frac{2}{3}$  indicates a structural unit that extends infinitely in two dimensions, i.e., a sheet.) The space between the compact sheets is filled with a thick open assemblage of  $\text{CaO}_5(\text{H}_2\text{O})_2$

\*E-mail: akampf@nhm.org

TABLE 1. Atomic coordinates and displacement parameters ( $\text{\AA}^2 \times 10^4$ ) for pararobertsite

	x	y	z	$U_{11}$	$U_{22}$	$U_{33}$	$U_{23}$	$U_{13}$	$U_{12}$	$U_{eq}$
Mn1	0	0	0	74(10)	112(10)	55(10)	12(9)	19(8)	-28(9)	79(4)
Mn2	0	0	1/2	108(10)	62(9)	49(10)	3(8)	28(8)	13(9)	72(4)
Mn3	0.0130(2)	0.1311(1)	0.2380(1)	86(6)	81(7)	54(6)	12(6)	16(5)	3(6)	73(3)
Mn4	0.0140(2)	0.2319(1)	0.4932(1)	69(7)	82(7)	54(8)	-7(6)	8(6)	-13(6)	69(3)
Ca1	0.3384(2)	0.3707(2)	0.5725(2)	84(8)	137(10)	214(10)	-08(9)	31(7)	-3(9)	145(4)
Ca2	0.6674(2)	0.1232(2)	0.3595(2)	106(8)	130(10)	123(9)	0(9)	2(7)	-15(9)	122(4)
P1	0.2968(3)	0.1104(2)	0.4457(2)	103(11)	71(12)	77(11)	15(9)	24(9)	-9(10)	83(5)
P2	0.0845(3)	0.1189(2)	0.7757(2)	112(11)	85(12)	100(11)	-15(10)	23(9)	-2(11)	99(5)
P3	0.7281(3)	0.1407(2)	0.0292(2)	63(10)	90(12)	67(11)	-7(9)	18(8)	-10(9)	73(5)
O1	0.4696(7)	0.1112(5)	0.4660(5)	128(32)	183(38)	92(31)	35(29)	7(25)	5(30)	136(14)
O2	0.2361(7)	0.2038(5)	0.5065(6)	62(32)	101(32)	79(33)	-17(26)	15(27)	22(26)	81(14)
O3	0.2344(8)	0.0125(5)	0.4985(6)	150(35)	41(32)	141(35)	6(27)	41(29)	-38(27)	109(14)
O4	0.2280(7)	0.1135(5)	0.3039(5)	109(30)	173(35)	58(29)	22(29)	0(24)	-12(30)	115(13)
O5	0.2558(7)	0.1180(5)	0.8283(6)	104(30)	143(35)	240(37)	-18(33)	30(27)	10(31)	163(14)
O6	0.0089(7)	0.2162(5)	0.8103(6)	136(34)	114(34)	130(35)	4(28)	77(28)	38(28)	120(14)
O7	0.0349(7)	0.1083(5)	0.6354(5)	146(32)	118(34)	74(30)	12(26)	27(26)	-25(28)	112(14)
O8	0.0021(7)	0.0302(5)	0.8293(6)	124(34)	70(32)	124(35)	16(26)	31(28)	2(27)	105(14)
O9	0.5574(7)	0.1429(5)	0.0003(6)	91(30)	196(39)	106(31)	-8(29)	43(25)	-41(29)	128(14)
O10	0.7949(7)	0.2359(5)	0.9754(6)	76(33)	92(32)	105(35)	29(26)	37(27)	-13(26)	88(14)
O11	0.7912(7)	0.1399(5)	0.1709(5)	96(29)	134(35)	44(29)	-17(26)	-2(24)	24(28)	93(13)
O12	0.7866(7)	0.0429(5)	0.9729(6)	66(33)	158(35)	86(35)	-71(27)	4(28)	-38(27)	105(15)
O13	0.9532(6)	0.1111(5)	0.3952(5)	87(29)	56(30)	72(29)	-14(26)	26(24)	32(27)	70(12)
O14	0.0678(7)	0.1490(5)	0.0797(5)	60(29)	148(36)	78(31)	24(26)	-4(24)	31(27)	98(14)
O15	0.5175(8)	0.0124(5)	0.2143(7)	220(41)	102(36)	198(38)	49(30)	29(32)	-2(30)	175(16)
O16	0.4783(8)	0.2372(5)	0.2383(6)	134(36)	172(39)	208(42)	-16(30)	13(31)	10(30)	174(17)
O17	0.6702(9)	0.3843(6)	0.1964(6)	462(48)	143(38)	217(38)	37(34)	172(35)	-27(39)	260(17)
H1	0.4311	0.9791	0.2406							5
H2	0.6035	0.9367	0.1929							5
H3	0.5446	0.2719	0.2463							5
H4	0.4150	0.2680	0.2482							5
H5	0.7146	0.3309	0.1885							5
H6	0.6275	0.4330	0.1204							5

polyhedra and isolated water molecules. The structure bears strong similarities to the mitridatite (robertsite) structure type.

The compact sheet of octahedra and tetrahedra in mitridatite (Fig. 1b) is based upon nine-membered trigonal rings of edge-sharing octahedra. While the ring motif in mitridatite represents a distinctly different topology from the Z-chain motif in pararobertsite, the local geometries of the octahedral linkages are similar in the two sheets. Furthermore, the loci of the trivalent cations in both of the sheets define the vertices of the Kagomé net (Figs. 1c and 1d). This latter structural similarity accounts for the similar pseudohexagonal symmetries noted by Roberts et al. (1989) in the *OkI* planes of precession films for these minerals. The linkings of  $\text{PO}_4$  tetrahedra to the octahedra in the two sheets are topologically and geometrically quite similar as well, leading to identical sheet compositions in the two structures. One interesting contrast between the sheets is that the geometry of the ring motif of mitridatite requires linkages of octahedra and tetrahedra that yield non-centric (polar) symmetry, while the Z-chain geometry of pararobertsite is consistent with a centric arrangement of octahedra and tetrahedra.

The two nonequivalent Ca atoms nestle into pockets in the sheets, each forming bonds to four phosphate O atoms and one oxo atom (also shared by three  $\text{Mn}^{3+}$  atoms in the sheet). The sevenfold coordination of each Ca is completed by bonds to

two water molecules. The water molecules define a shared edge between two Ca polyhedra nestled into adjacent sheets, thereby creating  $\text{Ca}_2\text{O}_{10}(\text{H}_2\text{O})_2$  dimers, which provide the glue that binds the sheets to one another. Contributing to a lesser extent to the adhesion between the sheets is a network of hydrogen bonds involving the water molecules bonded to the Ca atoms and an additional free water molecule also nestled into pockets in the sheets. The  ${}^{\infty}[\text{Ca}_2\text{O}_{10}(\text{H}_2\text{O})_2 \cdot \text{H}_2\text{O}]$  layer described above and shown in (Fig. 2) matches the corresponding layer in mitridatite very closely. Figure 3 shows the assembly of  ${}^{\infty}[\text{Mn}_3^+\text{O}_2(\text{PO}_4)_3]$  sheets and the  ${}^{\infty}[\text{Ca}_2\text{O}_{10}(\text{H}_2\text{O})_2 \cdot \text{H}_2\text{O}]$  layer on edge.

The structural formula for pararobertsite is  $\text{Ca}_2(\text{H}_2\text{O})_2[\text{Mn}_3^+\text{O}_2(\text{PO}_4)_3] \cdot \text{H}_2\text{O}$ ,  $Z = 4$ . This is consistent with the formula proposed by Roberts et al. (1989) and is exactly one third the cell content of robertsite,  $\text{Ca}_6(\text{H}_2\text{O})_6[\text{Mn}_9^+\text{O}_6(\text{PO}_4)_9] \cdot 3\text{H}_2\text{O}$ ,  $Z = 4$ . Not surprising from the structural similarities noted above is the fact that the cell volume of pararobertsite ( $1265.1 \text{ \AA}^3$ ) is almost exactly one third that of robertsite ( $3810.2 \text{ \AA}^3$ ).

### $\text{Mn}^{3+}\text{O}_6$ octahedra

Moore and Araki (1977) commented on the distortions of octahedra inherent in the edge-sharing nonamers and octahedral sheet as a whole in the mitridatite structure type. The *cis* edge-sharing octahedra (Fe1, Fe2, and Fe3) at the corners of the trigonal rings in mitridatite must be severely strained in order to achieve a Fe-Fe-Fe angle approaching  $60^\circ$ . It is intriguing that a virtually identically distorted *cis* edge-sharing octahedron (Mn4) is incorporated at the bends in the Z-chains of pararobertsite.

Cation-cation repulsions across the shared edges play a significant role in the geometries of the octahedra, effectively

<sup>1</sup>For a copy of Table 2, document item AM-00-048, contact the Business Office of the Mineralogical Society of America (see inside front cover of recent issue) for price information. Deposit items may also be available on the American Mineralogist web site (<http://www.minsocam.org>).

**TABLE 3.** Bond lengths (Å) and selected polyhedral edge lengths (Å) and bond angles (°) in pararobertsite

Mn1-O12 ×2	1.932		Mn2-O13×2	1.867		Ca1-O9	2.234	H1-O15-H2	103°
Mn1-O8 ×2	1.933		Mn2-O7 ×2	2.052		Ca1-O14	2.417	O15-H1	0.97
Mn1-O14 ×2	2.195		Mn2-O3 ×2	2.076		Ca1-O2	2.443	H1-O17	1.76
Mean	2.020		Mean	1.998		Ca1-O16	2.459	O15-H2	1.30
O8-O14 ×2*	2.693	81.2	O7-O13 ×2*	2.613	83.5	Ca1-O15	2.527	H2-O5	1.49
O8-O12 ×2	2.707	88.9	O3-O13 ×2	2.746	88.1	Ca1-O12	2.538		
O8-O12 ×2	2.758	91.1	O3-O7 ×2	2.832	86.6	Ca1-O5	2.660	H3-O16-H4	105°
O12-O14 ×2	2.894	88.8	O3-O13 ×2	2.837	91.9	Mean 2.468		O16-H3	0.73
O12-O14 ×2	2.954	91.2	O7-O13 ×2	2.926	96.5			H3-O17	1.99
O8-O14 ×2	3.139	98.8	O3-O7 ×2	3.003	93.4	Ca2-O1	2.291	O16-H4	0.72
Mean	2.858	90.0	Mean	2.826	90.0	Ca2-O15	2.377	H4-O5	2.35
						Ca2-O10	2.414		
Mn3-O4	1.908		Mn4-O14	1.857		Ca2-O3	2.431	H5-O17-H6	123°
Mn3-O14	1.918		Mn4-O13	1.948		Ca2-O16	2.447	O17-H5	0.82
Mn3-O13	1.931		Mn4-O10	1.950		Ca2-O13	2.478	H5-O11	2.63
Mn3-O11	1.955		Mn4-O2	1.970		Ca2-O11	2.544	H5-O6	2.75
Mn3-O6	2.176		Mn4-O6	2.128		Mean 2.426		H5-O10	2.88
Mn3-O8	2.255		Mn4-O7	2.252				O17-H6	1.07
Mean	2.024		Mean	2.018		P1-O1	1.496	H6-O1	2.07
O6-O13*	2.556	76.7	O6-O13*	2.556	77.5	P1-O2	1.552		
O11-O13	2.639	85.5	O7-O13*	2.613	76.6	P1-O3	1.564		
O4-O14	2.646	87.5	O2-O14	2.667	88.3	P1-O4	1.568		
O8-O14*	2.693	79.9	O10-O13	2.704	87.9	Mean 1.545			
O4-O13	2.799	93.7	O10-O14	2.713	90.9				
O11-O14	2.815	93.2	O2-O7	2.785	82.3	P2-O5	1.509		
O8-O11	2.896	86.6	O2-O13	2.837	92.8	P2-O6	1.531		
O6-O11	2.922	89.8	O2-O6	2.855	88.3	P2-O7	1.534		
O4-O8	2.955	90.1	O6-O10	2.880	89.7	P2-O8	1.558		
O4-O6	2.978	93.4	O6-O14	3.056	99.9	Mean 1.533			
O8-O13	3.192	99.1	O7-O10	3.226	100.1				
O6-O14	3.234	104.2	O7-O14	3.293	106.2	P3-O9	1.476		
Mean	2.860	90.0	Mean	2.849	90.0	P3-O10	1.556		
						P3-O11	1.558		
						P3-O12	1.566		
						Mean 1.539			

Notes: Standard deviations for bond distances are 0.006 to 0.007 for Ca,Mn,P-O and 0.008 to 0.009 for O-O. Standard deviations for bond angles are 0.2 to 0.4. Asterisks (\*) indicate shared octahedral edges. The number following each O-O distance denotes the corresponding O-M-O angle.

**TABLE 4.** Bond valences for pararobertsite

	O1	O2	O3	O4	O5	O6	O7	O8	O9	O10	O11	O12	O13	O14	O15	O16	O17	Σ <sub>v</sub>
Ca1		0.276			0.154				0.486			0.214		0.296	0.220	0.265		1.911
Ca2	0.417		0.285							0.299	0.210		0.251		0.330	0.273		2.066
Mn1								0.627 ×2			0.628 ×2	0.309 ×2			3.127			
Mn2			0.426 ×2			0.454 ×2						0.749 ×2				3.258		
Mn3				0.670		0.325	0.262				0.590		0.630	0.652				3.130
Mn4		0.567				0.370	0.265			0.598			0.602	0.769				3.171
P1	1.387	1.192	1.154	1.142														4.875
P2					1.339	1.262	1.251	1.173										5.025
P3									1.464	1.179	1.173	1.148						4.964
H1															0.790		0.210	1.000
H2					0.330										0.670			1.000
H3																0.870	0.130	1.000
H4				0.070												0.930		1.000
H5						0.030				0.020	0.040						0.910	1.000
H6	0.110																0.890	1.000
Σ <sub>a</sub> v	1.913	2.035	1.865	1.812	1.893	1.986	1.970	2.062	1.950	2.096	2.013	1.990	2.232	2.027	2.010	2.338	2.140	

Notes: Multiplicities are indicated for equivalent bonds for each cation. Constants from Brese and O'Keeffe (1991). Hydrogen bond valence based upon Brown and Altermatt (1985).

shortening the polyhedral shared O-O edges and diminishing the corresponding polyhedral angles (see Table 3). Again the distortions are most dramatically manifest in the Mn4 octahedron because its two shortest edges are adjacent. An interesting conjecture is that the Kagomé net arrangements of the M<sup>3+</sup> cations within the planes of octahedra in the mitridatite and pararobertsite sheets (Figs. 1c and 1d) developed in response to M<sup>3+</sup> cation-cation repulsions. This arrangement can be viewed as a planar cation close-packing with vacancies. In both structures P<sup>5+</sup> cations (P2 in pararobertsite) are located at sites slightly above or below the vacancies in the cation close-packed planes.

Note that the M<sup>3+</sup>-M<sup>3+</sup> distances are shortest across the shared edges (thicker lines in Figs. 1c and 1d).

The Mn1, Mn3, and Mn4 octahedra exhibit classic Jahn-Teller distortion, each having two long apical bonds, whereas the Mn2 octahedron shows a "reverse" Jahn-Teller distortion with two shortened apical bonds. Based upon bond valence considerations, Moore and Araki (1977) predicted the Jahn-Teller distortions that would be manifest in the structure of robertsite, the Mn<sup>3+</sup> analog of mitridatite. Their predictions were borne out with the solution of the lāngbanite structure (Moore et al. 1991), which includes, among four discrete sheets, a

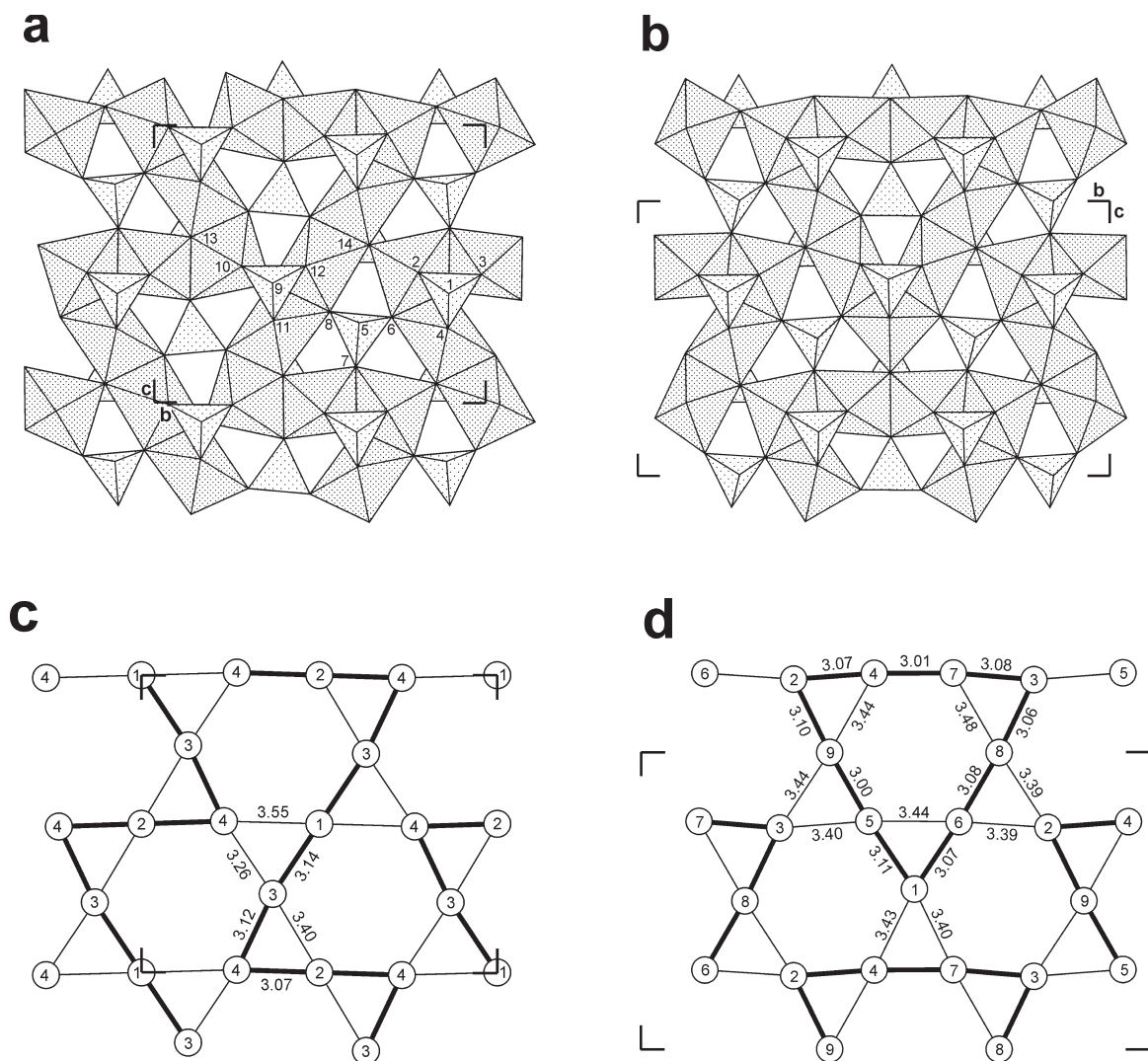


**FIGURE 1.** (a) Pararobertsite sheet of composition  $\sum_2[\text{Mn}^{3+}_2\text{O}_2(\text{PO}_4)_3]^+$  oriented parallel to  $\{100\}$ . The O atoms are numbered; Mn atoms can be identified from Figure 1c. P1, P2, and P3 can be identified by their bonded O atoms. (b) Mitridatite sheet of composition  $\sum_2[\text{Fe}^{3+}_3\text{O}_6(\text{PO}_4)_9]^{12-}$  oriented parallel to  $\{100\}$ . (c) Kagomé net of  $\text{Mn}^{3+}$  atoms in pararobertsite.  $\text{Mn}^{3+}$ - $\text{Mn}^{3+}$  distances are shown; distances corresponding to shared edges are indicated by thick lines. (d) Kagomé net of  $\text{Fe}^{3+}$  atoms in mitridatite. For 1c and 1d,  $\text{M}^{3+}$ - $\text{M}^{3+}$  distances are shown; distances corresponding to shared edges are indicated by thick lines.

mitridatite-type sheet of  $\text{Mn}^{3+}$  octahedra. The Jahn-Teller distortions in the Mn3 and Mn4 octahedra in pararobertsite correspond to the distortions observed in similarly positioned octahedra in the mitridatite-type sheet of lāngbanite. All of the elongated apical bonds in these octahedra and in the Mn1 octahedron are in the plane of the sheet. The shortened apical bond pair of the Mn2 octahedron is also in this plane. This suggests a complimentary relationship between the Jahn-Teller distortions and the distortions required by the geometry of the octahedral linkages within the sheets. Of course, the bond valence balance is an essential component of this relationship.

A final consideration in assessing the distortions of the octahedra is the canting of the octahedral vertices that are not in

the plane of the sheet. This canting is necessary to accommodate the linkages to the  $\text{PO}_4$  tetrahedra (P1 and P3).

Besides exhibiting a reverse Jahn-Teller effect, the Mn2 octahedron shows the least O-Mn-O angular distortions and has the shortest Mn-O average bond distance, 1.998 Å. This is also shorter than any octahedral Fe-O average noted in mitridatite. It is likely that the small quantity of  $\text{Fe}^{3+}$  in pararobertsite reported by Roberts et al. (1989) is accommodated in this site.

#### **$\text{PO}_4$ tetrahedra**

Each of the three nonequivalent  $\text{PO}_4$  tetrahedra possesses one P-O bond that is significantly shorter than the rest. The

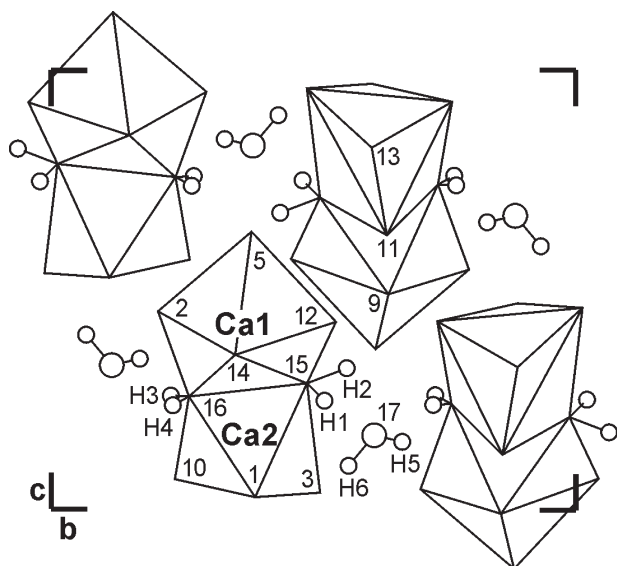


FIGURE 2. A  $\frac{1}{2}$ [Ca<sub>2</sub>O<sub>10</sub>(H<sub>2</sub>O)<sub>2</sub>·H<sub>2</sub>O] layer in pararobertsite oriented parallel to {100}. The O and H atoms are numbered.

same is observed in the mitridatite structure. In every case in both structures, the short P-O bond points away from the plane of the octahedral sheet and is not involved in any M<sup>3+</sup> bonds. Each of these O atoms bonds only to one P and one Ca atom (sometimes with H bonding as well), and the short P-O bonds compensate for the otherwise relatively low bond strength sums received by these O atoms.

#### CaO<sub>5</sub>(H<sub>2</sub>O)<sub>2</sub> polyhedra

Both of the two nonequivalent Ca atoms in pararobertsite are coordinated to seven O atoms: four from phosphate groups, one in the plane of the octahedral sheet, and two of H<sub>2</sub>O molecules. The coordination geometry about Ca1 is irregular, while that about Ca2 can be described as an octahedron with an additional oxygen above one octahedral face (e.g., a monocapped octahedron). The latter geometry is comparable to that noted for all of the Ca polyhedra in mitridatite.

#### ACKNOWLEDGMENTS

Structure data collection and analysis were performed in the X-ray Crystallography Laboratory of the University of California, Los Angeles, Department

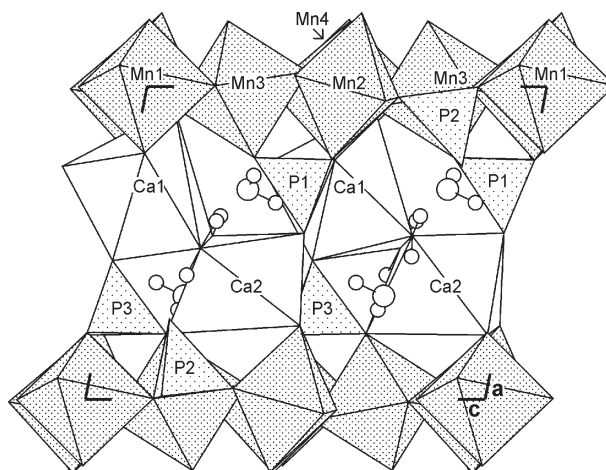


FIGURE 3. Atomic structure of pararobertsite viewed down the *b* axis. Octahedra have a medium stipple. Tetrahedra are lightly stippled. H<sub>2</sub>O molecules are shown in perspective.

of Chemistry and Biochemistry. Saeed Khan of that laboratory is acknowledged for technical assistance. Eric Fritsch provided the crystal used in this study from the collection of the South Dakota School of Mines and Technology. Paulus B. Moore is gratefully acknowledged for his valuable insights.

#### REFERENCES CITED

- Breese, N.E. and O'Keeffe, M. (1991) Bond-valence parameters for solids. *Acta Crystallographica*, B47, 192–197.
- Brown, I.D. and Altermatt, D. (1985) Bond-valence parameters obtained from a systematic analysis of the inorganic structure database. *Acta Crystallographica*, B41, 244–247.
- Moore, P.B. and Araki, T. (1977) Mitridatite, Ca<sub>6</sub>(H<sub>2</sub>O)<sub>6</sub>[Fe<sup>III</sup><sub>9</sub>O<sub>6</sub>(PO<sub>4</sub>)<sub>6</sub>]-3H<sub>2</sub>O. A noteworthy octahedral sheet structure. *Inorganic Chemistry*, 16, 1096–1106.
- Moore, P.B., Sen Gupta, P.K., and Le Page, Y. (1991) The remarkable langbanite structure type: Crystal structure, chemical crystallography, and relation to some other close-packed structures. *American Mineralogist*, 76, 1408–1425.
- Roberts, A.C., Sturman, B.D., Dunn, P.J., and Roberts, W.L. (1989) Pararobertsite, Ca<sub>2</sub>Mn<sup>3+</sup>(PO<sub>4</sub>)<sub>3</sub>O<sub>2</sub>·3H<sub>2</sub>O. *Canadian Mineralogist*, 27, 451–455.
- Sheldrick, G.M. (1997) SHELXL97. Program for the refinement of crystal structures. University of Göttingen, Germany.

MANUSCRIPT RECEIVED DECEMBER 21, 1999

MANUSCRIPT ACCEPTED APRIL 3, 2000

PAPER HANDLED BY YANBIN WANG